Scientia Iranica A (2014) 21(2), 318–328

Sharif University of Technology
Scientia Iranica
Transactions A: Civil Engineering
www.scientiairanica.com

Lattice Boltzmann method for simulating impulsive water waves generated by landslides

A. Pak* **and M. Sarfaraz**

Department of Civil Engineering, Sharif University of Technology, Tehran, P.O. Box 11155-9313, Iran.

Received 6 April 2013; received in revised form 6 July 2013; accepted 27 July 2013

KEYWORDS
Lattice Boltzmann method;
Impulsive water waves;
Landslides;
Free surface flow;
Numerical modeling.

Abstract. Impulsive water waves generated by landslides impose severe damage on coastal areas. Very large mass flows in the ocean can generate catastrophic tsunamis. Preventing damage to dams and coastal structures, and saving the lives of local people against landslide-generated waves, has become an increasingly important issue in recent years. Numerical modeling of landslide-generated waves is a challenging subject in CFD. The reason lies in the difficulty of determining the interaction between the moving solids and sea water, which causes complicated turbulent regimes around the moving mass and at the water surface. Submarine or aerial types of landslide can further complicate the problem. Up to now, a number of numerical approaches have been proposed for predicting the behavior of flow during and after mass movement. In this study, a Lattice Boltzmann Method (LBM) based-code is employed for analyzing and simulating the impulsive water waves generated by landslides. Four experimental cases of submerged and aerial landslides have been modeled to investigate the efficiency and accuracy of the LBM code, and the obtained results are verified against experimental observations. The results indicate the capability of LBM in simulating complicated flow fields and demonstrate its superiority over numerical methods used so far, such as SPH and RANS.

1. Introduction

Impulsive water waves generated by aerial or submerged landslides can exert considerable damage on coastal areas. These landslides frequently occur in dam reservoirs, lakes, and oceans. Saving the lives of local people and reinforcing the structures in these areas, because of the detrimental effects of impulsive waves, has turned into a major issue for coastal authorities.

A number of laboratory tests have been conducted to study aerial and submerged landslides, e.g. Heinrich [1], Walder et al. [2], Fritz et al. [3], Grilli and Watts [4], Panizzo et al. [5], and Ataie and Najafi [6]. Studies show that a complex nonlinear interaction occurs between the surface waves and the motion of the sliding body.

Until now, two major numerical schemes have been utilized to model impulsive waves generated by landslides. The first class contains the conventional CFD method, founded on solving Navier-Stokes and VOF equations, which is an Eulerian and macroscopic approach. Rzadkiewicz et al. [7], Titov [8], Imran et al. [9], and Pak and Sarfaraz [10] are some examples of applying this method.

This method has some drawbacks when it is used to simulate the severe interaction between water and sliding material. The VOF scheme adds an additional transport equation and an artificial diffusion to the interface profile [11]. Coupling fluid flow with the moving boundaries of the sliding block is challenging and difficult using the Eulerian method [12]. Also,

*. *Corresponding author. Tel.: +98 21 6616 4225*
E-mail addresses: pak@sharif.edu (A. Pak); sarfaraz@alum.sharif.edu (M. Sarfaraz)

this method suffers from instability, extensive computational time and poor scalability [13].

In the second approach, SPH, a macroscopic scheme, is employed to model the motion of the landslides in water. Due to its Lagrangian scheme, it has been used vastly by researchers in studying landslides, e.g. Monaghan and Kos [14], Gotoh et al. [15], Lo and Shao [16], Shao and Lo [17], Shao and Gotoh [18], Ataie and Shobeyri [19], and Mansour-Rezaei and Ataie [20].

The stability, accuracy, and speed of SPH depend on its smoothing kernel, which should be chosen carefully for each specific problem [13,21]. In particular, a unique kernel function has not been proposed as suitable for all landslide problems, including different geometrical and physical parameters [19]. Incompressibility cannot be strictly assured in commonly used SPH codes, because, in these codes, a relation between pressure and density is assumed [13]. Boundaries are not modeled well in SPH. The particles at the edge of the objects have no neighbors outside, so, their densities are less than those of internal particles [22]. In most of the developed codes, e.g. [19,20,23], SPH was not used to model the landslide motion through a fully-coupled interaction with water, i.e. a prescribed relation obtained by physical tests was implemented for the velocity of the solid. Yim et al. [23] reported that the accuracy of SPH was less than that of the Eulerian approach.

Apart from the Eulerian and SPH approaches, the Lattice Boltzmann Method (LBM) has become proficient in solving a variety of complex and difficult fluid dynamic problems over the last 15 years. The fundamental idea of the LBM is to construct simplified kinetic models that incorporate the essential physics of microscopic or mesoscopic processes, so that the microscopic averaged properties obey the desired macroscopic equations [24].

In LBM, the spatial space is discretized in such a way that it is consistent with the kinetic equation. LBM is a mesoscopic model simulating flow phenomenon through tracking fluid particle packs that move and collide in space under the rules in which collision does not result in mass and momentum changes [25]. Space is divided into regular lattices and, at each lattice site, a particle distribution function, f_α, is defined, which is equal to the expected number of particles of fluid in the direction of α. During each discrete time step of the simulation (Δt), fluid particles move to the nearest lattice site along their direction of motion, with different velocities of e_α, where they "collide" with other fluid particles that arrive at the same site. The outcome of the collision is determined by solving the kinetic (Boltzmann) equation for the new particle distribution function at that site, and the particle distribution function is updated [24].

LBM has been employed to model complicated flow, such as turbulent and free surface flows, accurately [26,27]. The parallelism of the algorithm, simplicity of programming and possibility of modeling complex geometrical flow problems are remarkable advantages of LBM [27]. A single LB time-step is significantly faster than a single step of an Eulerian solver [13]. Hence, time dependent flow modeling is straightforward, especially in 3D, whereas it is costly in the Eulerian approach [25]. Also, LBM exhibits good stability for unsteady problems [27].

This paper aims to simulate impulsive waves generated by aerial and submarine landslides, using LBM to exhibit its accuracy and efficiency in modeling this complicated free-surface problems. According to the authors' knowledge, this is the first research that uses LBM to simulate the impulsive waves generated by landslides.

2. Numerical formulation

In this paper, the Single Relaxation Time (SRT) approximation with the Bhantager-Gross-Krook (BGK) collusion rule is adopted to discretize the Boltzmann equation. For the D2Q9 model (Figure 1), it is given by [28]:

$$f_\alpha(\vec{x_i} + \vec{e_\alpha}\delta t, t + \Delta t) - f_\alpha(\vec{x_i}, t) = -\frac{f_\alpha(\vec{x_i}, t) - f_\alpha^{\mathrm{eq}}(\vec{x_i}, t)}{\tau} + F_\alpha, \tag{1}$$

where x_i, e_α, Δt, f_α, f_α^{eq} and F_α are the position of the point in the discretized space, the discrete particle velocity, the time step, the distribution function, the corresponding equilibrium distribution function and the body force (e.g. gravity) function, respectively.

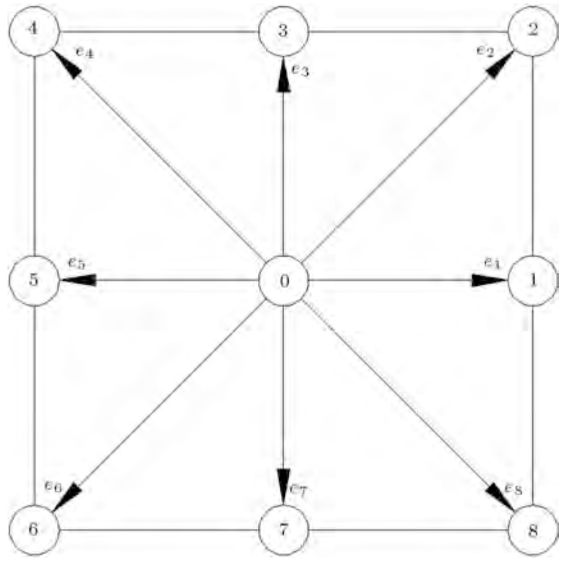

Figure 1. D2Q9 lattice scheme.

To satisfy the incompressible flow limit, according to the Navier-Stokes equation, by adopting the Chapman-Enskog expansion, the relaxation time (τ) is related to the fluid viscosity (ν), as [29]:

$$\upsilon = \frac{1}{3}(\tau - \frac{1}{2})\Delta t. \tag{2}$$

The equilibrium distribution is of the form [29]:

$$f_\alpha^{\text{eq}} = \rho\omega_\alpha \left(1 + 3\vec{e_\alpha}.\vec{u} + 4.5(\vec{e_\alpha}.\vec{u})^2 - 1.5\vec{u}.\vec{u}\right), \tag{3}$$

where u is the fluid velocity, and ω_α is defined as:

$$\omega_\alpha = \begin{cases} 16/36 & \alpha = 0 \\ 4/36 & \alpha = 1,3,5,7 \\ 1/36 & \alpha = 2,4,6,8 \end{cases} \tag{4}$$

Gravity vector (g) for free surface modeling is considered as [30]:

$$F_\alpha = 3\omega_\alpha\rho[(\vec{e_\alpha} - \vec{u}) + (\vec{e_\alpha}.\vec{u})\vec{e_\alpha}].\vec{g}. \tag{5}$$

Density (ρ) and momentum fluxes (ρu) are evaluated by:

$$\rho = \sum_{\alpha=0}^{8} f_\alpha = \sum_{\alpha=0}^{8} f_\alpha^{\text{eq}}, \tag{6}$$

$$\rho\vec{u} = \sum_{\alpha=0}^{8} \vec{e_\alpha} f_\alpha = \sum_{\alpha=0}^{8} \vec{e}_\alpha f_\alpha^{\text{eq}}. \tag{7}$$

For three-dimensional problems in this study, the D3Q19 model was implemented. The reader is referred to [11] for related formulation.

Due to the highly turbulent nature of the flow field generated by landslides, it is necessary to use a turbulence model. The role of this procedure is to parameterize the turbulent energy dissipation, where larger eddies extract energy from the mean flow and transfer some of it to smaller eddies [31]. In this paper, the Wall-Adapting Local Eddy-viscosity (WALE), an LES category, is adopted. This model has good properties both near to and far from the wall, with laminar and turbulent flows. This model recovers the asymptotic behavior of the turbulent boundary layer when this layer can be directly solved, and it does not add artificial turbulent viscosity in the shear regions out of the wake. The WALE model is formulated as [32]:

$$\tau = 3\left(\upsilon + C_t^2\Delta^2\overline{\phi}\right) + 0.5, \tag{8}$$

where C_t is equal to 0.5 and Δ denotes the filter width, which is set to lattice spacing (resolution). $\overline{\phi}$ is described as:

$$\overline{\phi} = \frac{(g_{i,j}g_{i,j})^{1.5}}{(S_{i,j}S_{i,j})^{2.5}(g_{i,j}g_{i,j})^{1.25}}, \tag{9}$$

$$g_{i,j} = S_{i,k}S_{k,j} + \Omega_{i,k}S_{k,j} - \frac{1}{3}\delta_{i,j}(S^2 - \Omega^2). \tag{10}$$

The shear stress tensor (S) and rotational stress tensor (Ω) are described as:

$$S_{i,j} = \upsilon\rho\left(\frac{\partial\overline{u_i}}{\partial x_j} + \frac{\partial\overline{u_j}}{\partial x_i}\right), \tag{11}$$

$$\Omega_{i,j} = \upsilon\rho\left(\frac{\partial\overline{u_i}}{\partial x_j} - \frac{\partial\overline{u_j}}{\partial x_i}\right), \tag{12}$$

where $\overline{u}$ is the spatially-filtered velocity calculated by [33]:

$$\overline{u}(x) = \int u(x)G(x,x')dx', \tag{13}$$

$$G(x,x') = \begin{cases} \Delta^{-1}, & |x - x'| \leq 0.5\Delta \\ 0, & \text{otherwise} \end{cases} \tag{14}$$

In this work, a central difference scheme is implemented to compute S and Ω, as proposed by Weickert et al. [32].

There are different proposed ways to model free surface flows in LBM [34-36]. In this study, the model presented by Körner et al. [36] is used, in which, the movement of the fluid interface is tracked by calculation of the mass contained in each lattice. This requires two additional values to be stored for each lattice: mass, m, and fluid fraction, ε. The fluid fraction is computed with lattice mass and density:

$$\varepsilon = m/\rho. \tag{15}$$

As the particle distribution functions correspond to a certain number of particles, the change of mass is directly computed from the values that are streamed between two adjacent lattices for each of the directions in the model. For an interface lattice (partially filled) and a fluid lattice at ($x + \Delta t\ e_\alpha$), this is given by:

$$\Delta m_\alpha(\vec{x}, t + \Delta t) = \tilde{f}_\alpha(\vec{x} + \Delta t\ \vec{e_\alpha}, t) - f_\alpha(\vec{x}, t). \tag{16}$$

The first particle distribution function is the amount of fluid entering this lattice in the current time step, and the second one is the amount leaving the lattice.

The mass exchange for two interface lattices has to take into account the area of the fluid interface between the two lattices. It is approximated by averaging the fluid fraction values of the two lattices.

Thus, Eq. (16) becomes:

$$\Delta m_\alpha(\vec{x},t+\Delta t) =\{\tilde{f}_\alpha(x+\Delta t\ \vec{e_\alpha},t) - f_\alpha(\vec{x},t)\}$$
$$\frac{\varepsilon(\vec{x}+\Delta t\ \vec{e_\alpha},t)+\varepsilon(\vec{x},t)}{2}. \quad (17)$$

For interface lattices with neighboring fluid lattices, the mass change has to conform to the particle distribution functions exchanged during streaming, as fluid lattices do not require additional computation. Their fluid fraction is always equal to one, and their mass equals their current density. The mass change values for all directions are added to the current mass for interface lattices, resulting in the mass for the next time step:

$$m(\vec{x},t+\Delta t) = m(\vec{x},t) + \sum_\alpha \Delta m_\alpha(\vec{x},t+\Delta t). \quad (18)$$

For more details, see [36,37].

For all cases in this work, the no-slip boundary condition (so-called the bounce-back rule) is used. The basic idea is that the incoming distribution functions at a wall node are reflected back, and rotated by π radians. The improvement suggested by Ziegler [38] was employed, considering the wall-fluid interface to be located halfway between the wall and fluid nodes, which has second-order accuracy for straight walls [29].

By using this rule, during the streaming step, the distribution functions are reflected at the obstacle surface. The stream step can be written as Eq. (19) for lattices where the neighbor at $x+e_\alpha$ is located as an obstacle:

$$f_\alpha(\vec{x},t+\Delta t)' = f_{\tilde{\alpha}}(\vec{x},t), \quad (19)$$

where $f_{\tilde{\alpha}}$ denotes the distribution function along the inverse velocity vector of f_α, therefore $e_{\tilde{\alpha}} = -e_\alpha$.

For moving obstacles (landslide blocks), the momentum of the movement should be transferred to the fluid. For this purpose, an additional forcing term is added to Eq. (19) during streaming:

$$f_\alpha(\vec{x},t+\Delta t)' = f_{\tilde{\alpha}}(\vec{x},t) + 6\omega_\alpha \rho \vec{e_\alpha}.\vec{u_0}, \quad (20)$$

where u_0 is the obstacle velocity at the obstacle boundary.

The momentum exchange method was utilized to compute the exerted fluid-forces to the landslide block. The total force is computed by [29]:

$$\vec{F} = \sum_{\text{all } x_b}\sum_{\alpha=1}\vec{e}_{\tilde{\alpha}}\left(\tilde{f}_\alpha(\vec{x_b},t)+\tilde{f}_{\tilde{\alpha}}(\vec{x_b}+\vec{e}_{\tilde{\alpha}}\Delta t,t)\right)$$
$$\times(1-W_f^b)\Delta x/\Delta t, \quad (21)$$

where x_b denotes lattice nodes on the solid side and $e_{\tilde{\alpha}}$ is the bounce-back particle velocity. $\tilde{f}_\alpha$ stands for post-collision distribution function. W_f^b is an indicator, which is 0 at lattice nodes on the fluid side next to the solid boundary and is 1 at x_b.

By using Eq. (20), fluid to obstacle coupling is computed, while its combination with Eq. (21) enables full two-way coupled fluid simulations that can be applied to study the landslide movement inside water. It is noted that the applied force to the obstacle, by applying Eq. (21), is used in Newton's second law to compute the obstacle velocity (u_0) in Eq. (20).

The aforementioned formulae are coded in the software, XFlow [39], that is used in this study.

3. Validation test cases

In this part, four physical tests are simulated by the LBM code. The experimental work includes both aerial and submerged rigid landslides. The tests were also numerically modeled using the Eulerian or SPH methods by other researchers, and are compared with the results of LBM.

3.1. 2D Submerged landslide (Heinrich [1])

The work was done in a flume of 20 m long and 0.5 m wide. A triangular rigid wedge with a density of 2036.4 kg/m^3 and a cross section area equal to 0.125 m^2 was allowed to slide freely on an inclined frictionless shoreline of 45° to horizontal. Water depth was 1.0 m and the wedge was initially 1.0 cm below the water surface. Figure 2 demonstrates the initial physical model configuration. The computational domain was the same as the physical model and a resolution (lattice dimension) of 0.03 m was used.

Pak and Sarfaraz [10] numerically modeled this case using FLOW-3D software. They applied three turbulence models of standard $k-\varepsilon$, RNG $k-\varepsilon$, and LES, and reported that LES results were more accurate.

In Figure 3, experimental surface wave profiles are demonstrated and compared with LBM results. Also, the numerical results of this problem, using the Eulerian approach by Pak and Sarfaraz [10], and applying the LES turbulence model, are included and compared. The figure shows that the LBM-based code

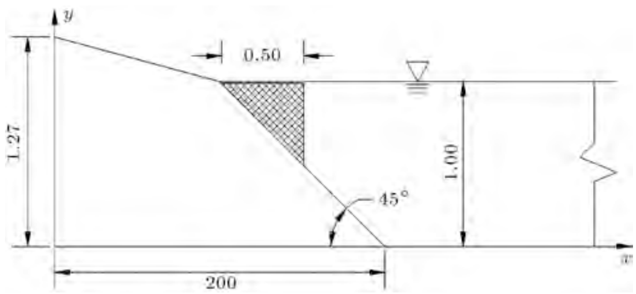

Figure 2. Initial configuration of the experimental work, case 1 (in meters).

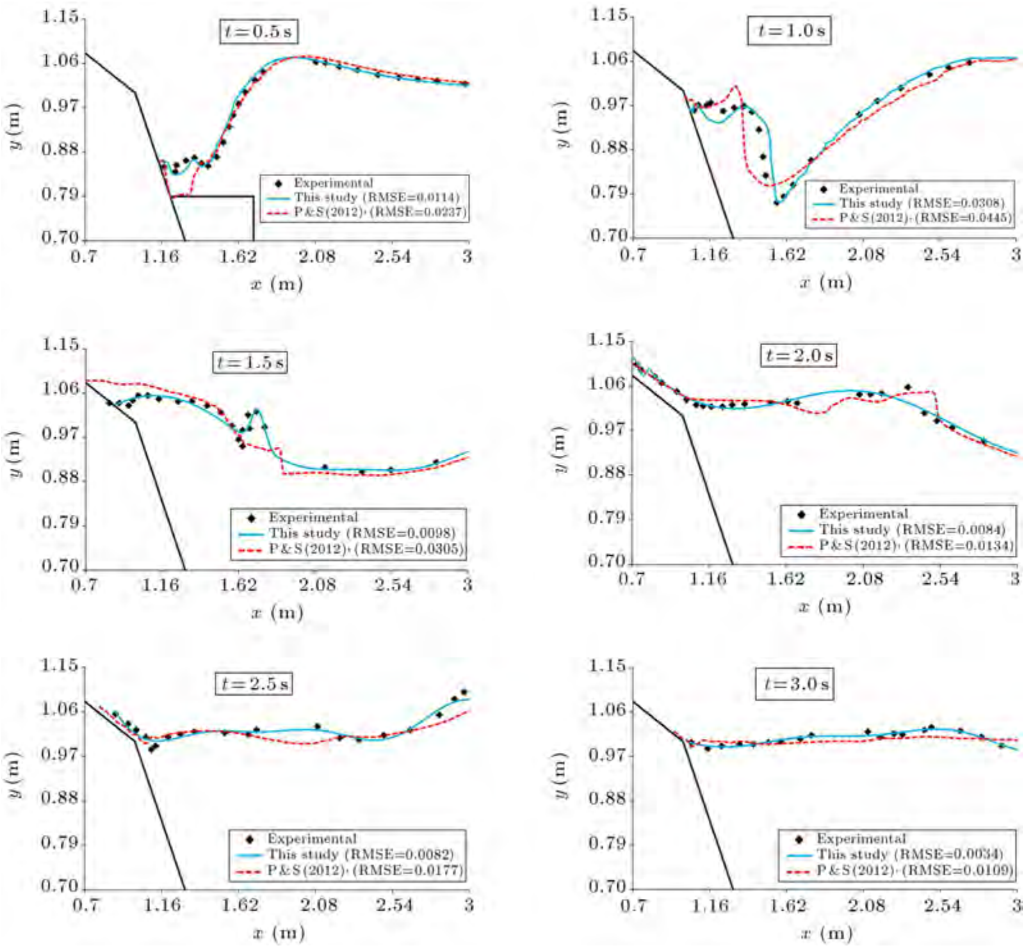

Figure 3. Experimental and numerical wave profiles at different times, case 1.

is successful and capable of tracking wave generation, due to the movement of the solid wedge, and is more accurate than the Eulerian results, according to its lower RMSE (Root Mean Square Error) values. Also, LBM proves its accuracy in capturing the configuration of highly turbulent flow near the beach.

Figure 4 displays and compares experimental and numerical wave amplitudes at $x = 4$, 8, 12 m over time. It is understood that LBM is well capable of predicting wave propagation due to the movement of the solid wedge in water. RMSE values indicate that the LBM-based code is more accurate than the Eulerian approach for computing the time history of free surface elevation due to wave propagation.

As indicated in the introduction section, equations within the Eulerian approach are complex and consist of high-order derivation terms, whose discretization will generate numerical errors. LBM can overcome these issues, as it contains a simple formulation and is straightforward in coupling the flow field with moving obstacles. Furthermore, LBM does not suffer from numerical issues such as instability. So, in this validation case, LBM provides more accurate results than the Eulerian technique.

In Figure 5, the velocity field and assigned vectors are presented at different times, showing the stability of the model in simulating the problem after the time at which the wedge has reached the bottom. As the wave propagates towards the right, a clockwise vortex is generated above the wedge, which resists coming down the run-up water. Also, the maximum velocity magnitude of these vortexes decreases over time.

3.2. 2D Partially submerged landslide (Yim et al. [23])

In this section, a solitary wave generated by the vertical falling of a partially submerged block into water (so-called Scott Russell's wave generator) is considered, and was carried out both physically and numerically (RANS and SPH) by Yim et al. [23]. The experiment was performed in a 12 m long flume, with a rectangular rigid block weighted 13.3 kg per width, having dimensions of 0.1 m. The flume contained 0.1 m depth of water and the bottom of the block was initially 3 cm below the still water level (Figure 6). The computational domain was the same as the physical model and a resolution of 4 mm was selected for lattices. The dynamic coefficient of friction between

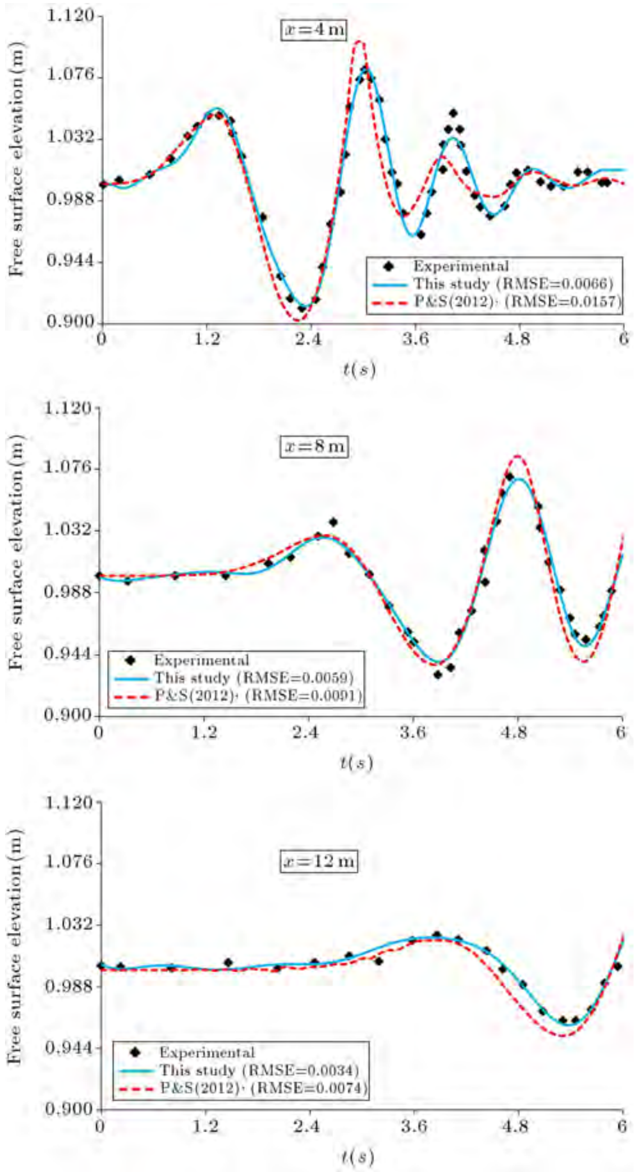

Figure 4. Experimental and numerical time history of wave amplitudes at different locations, case 1.

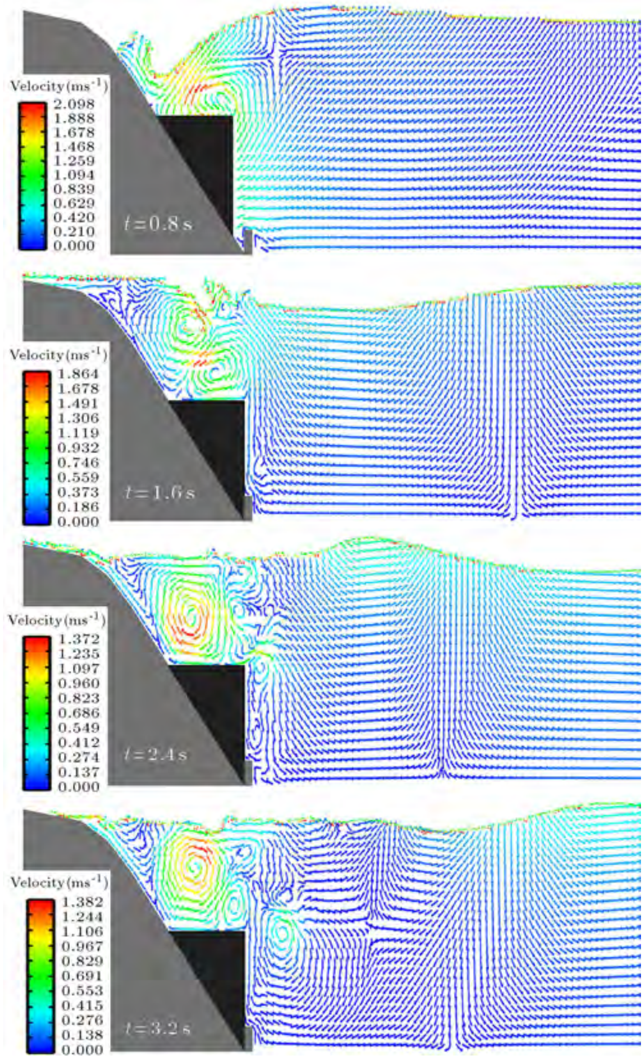

Figure 5. Velocity field with vectors at different times, case 1.

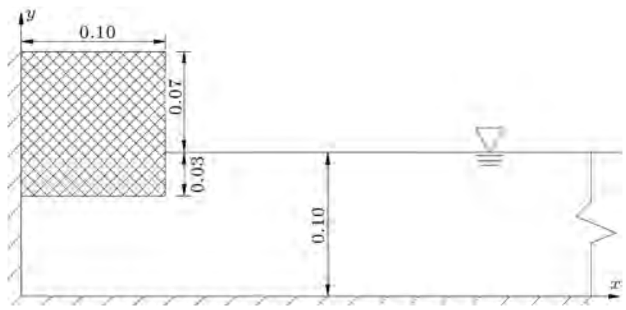

Figure 6. Initial configuration of experimental work, case 2 (in meters).

the block and vertical walls of the flume was equal to $\mu_d = 0.66$, as proposed in [23].

Figure 7 displays the experimental and computational position of the block mass center (y_{CG}). The RANS simulation by Yim et al. [23] was not stable after the block reached the bottom of the flume. Also, experimental values of y_{CG} were used in their SPH code for tracking the motion of the block. This figure indicates very good agreement between the LBM results and experimental data. The figure displays that the block does not meet the bottom of the flume for a time less than 1 s, which may be due to selecting a large friction coefficient.

The computational and experimental time history of free surface elevation at $x = 0.4$ and 0.85 m are shown in Figure 8. This figure shows that the wave propagates like a solitary wave, and RMSE values show that LBM is more accurate than SPH and RANS in predicting both the amplitude and phase of the wave. However, because of assuming a smooth surface for the flume bed, the simulated wave propagates slightly faster with slightly higher amplitude.

As it was explained before, boundaries are not

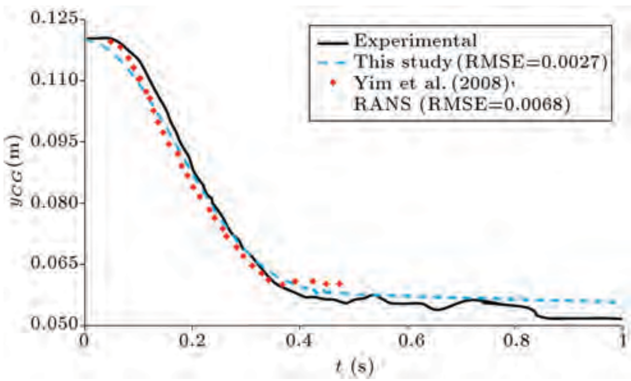

Figure 7. Experimental and computational time history of mass center position of block, case 2.

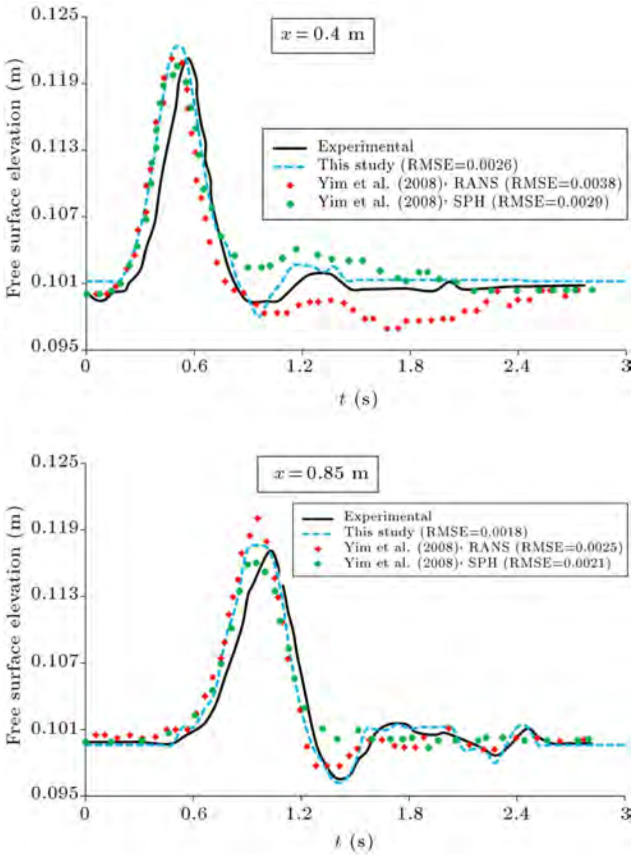

Figure 8. Experimental and computational time history of free surface elevation, case 2.

usually modeled well in SPH. Also, in common SPH codes, flow incompressibility cannot be guaranteed. Selecting an appropriate smoothing kernel is essential for the accuracy and stability of this method and is not unique for all landslide problems. Unlike the SPH method, boundaries are modeled in a logical way in LBM. Moreover, it does not need user-dependent parameters, e.g. smoothing kernel functions, and, therefore, LBM provides more accurate results in comparison with SPH.

The location of the falling block, with the velocity

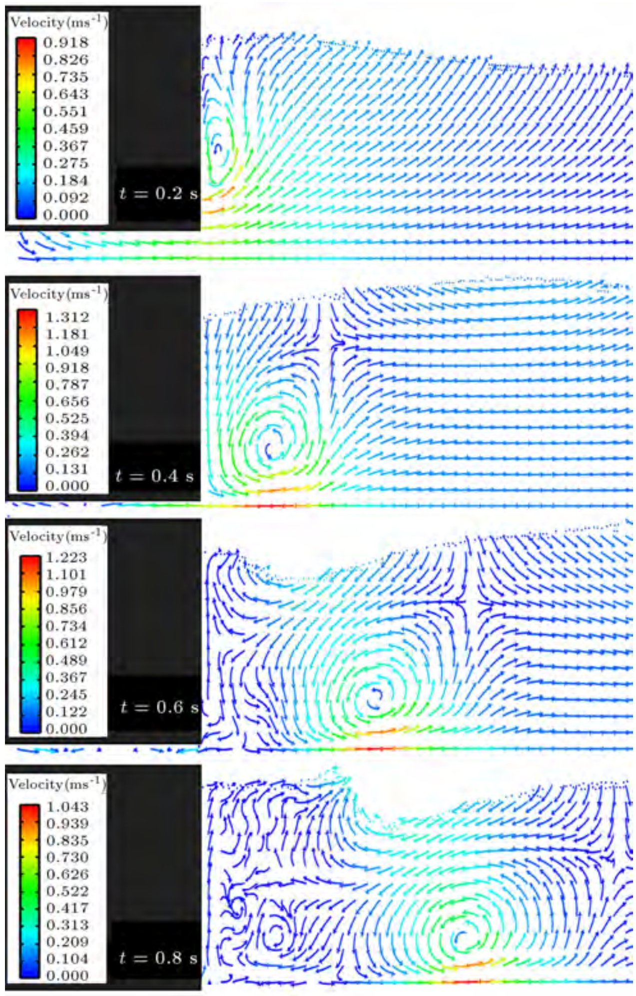

Figure 9. Velocity field with vectors at different times, case 2.

field and vectors, are presented in Figure 9 for different times. While the block is falling, a counterclockwise vortex develops near the right face of the block and is advected downstream with a slower speed than the phase speed of the generated wave. When the block reaches the bottom, the velocity magnitude tends to decrease and some small vortexes appear, caused by interaction between the propagated wave and run-up water near the block.

3.3. 2D Aerial landslide (Yim et al. [23])

The same materials and method as in the previous case are used in this case, except that the block was kept 3 cm initially above the still water with a depth of 0.18 m in the flume. Figure 10 shows the experimental and computed mass center position of the block, which exhibits good agreement between LBM results and experimental data. Before the block meets water, no friction was assumed in the code; hence, it compensates the large μ_d selected in the previous case.

The amplitudes and phase of the generated wave are well computed by LBM at $x = 0.4$ and 0.85 m

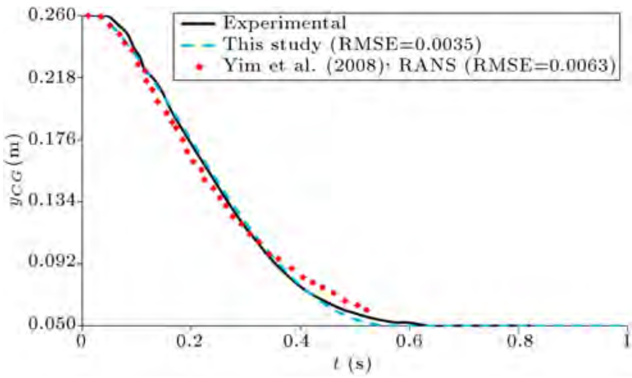

Figure 10. Experimental and computational time history of mass center position of block, case 3.

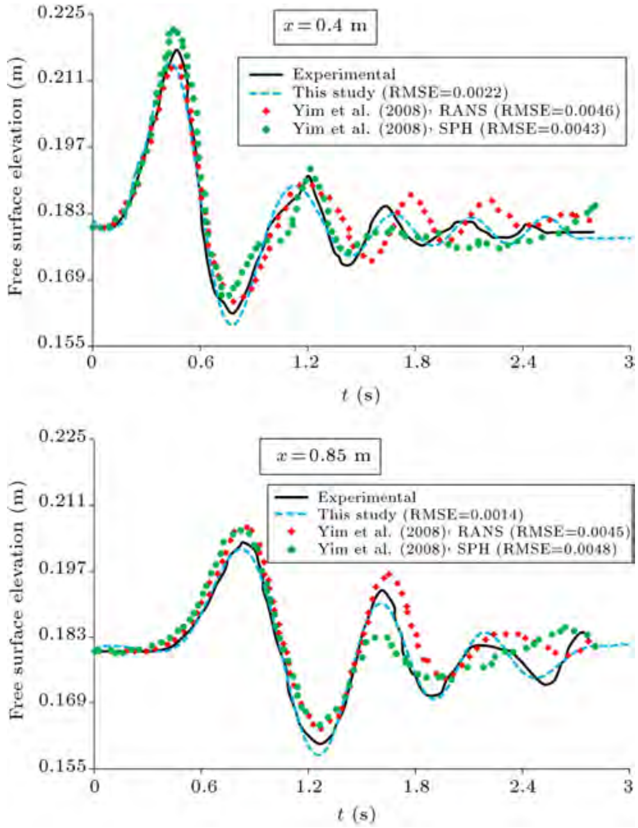

Figure 11. Experimental and computational time history of free surface elevation, case 3.

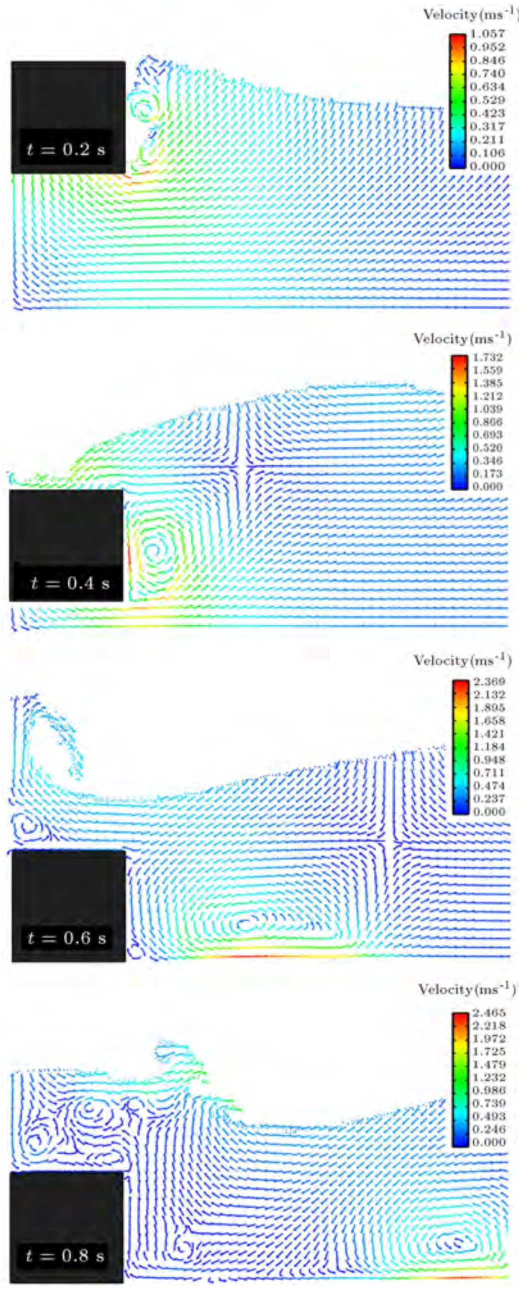

Figure 12. Velocity field with vectors at different times, case 3.

(see Figure 11). It is worth noting that since the still water depth is more than in the previous case, bed friction has less effect on the propagated wave; the phase difference between LBM and experimental data is negligible. There exists noticeable disagreement between the experimental and computed results by RANS and SPH after $t = 1.5$ s.

Figure 12 depicts the block location at different times, together with the velocity field and vectors. In view of the fact that the still water depth is more than the block height, water overtops the block, and then reflects back towards the flume. Since the block accelerates before going through the water, flow separation is observed near the right end of the block at $t = 0.2$ s. Similar to the previous case, a counterclockwise vortex appears and is advected with wave propagation, but is more stretched along the flume direction.

3.4. 3D Submerged landslide (Ataie and Najafi [6])

This part discusses the applicability and efficiency of the LBM method for modeling $3D$ landslide problems. A rigid rectangular block, with a weight of 14.82 kg, 0.3 m in length, 0.2 m in width and 0.13 m in height, was submerged initially on a 30° sloping beach with a 0.5 m depth of still water (see Figure 13). All surfaces were lubricated to eliminate friction and the test was repeated two times. The flume width was 2.5 m; therefore, it simulates a 3D landslide, as happens in the real world. In this experimental work, water elevation towards the centerline of the flume (along the x axis) was measured at different positions [6].

The computational domain was the same as the physical model, and a resolution of 8 mm was selected. Mansour-Rezaei and Ataie [20] simulated the same problem using SPH in the 3D space using different kernel functions. Experimental and computational values of free surface elevation at $x = 1.13$ and 2.03 m are shown in Figure 14. It is proved that LBM successfully overcomes the problems encountered to model the propagated wave in both amplitude and speed.

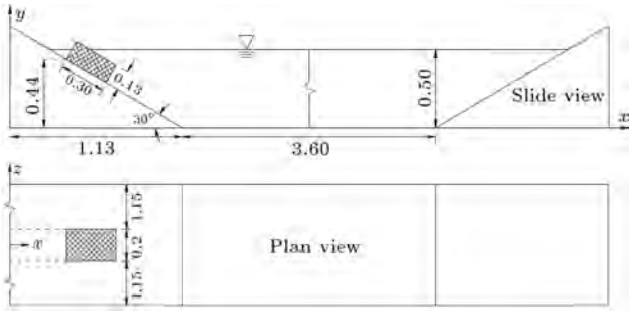

Figure 13. Initial configuration of experimental work, case 4 (in meters).

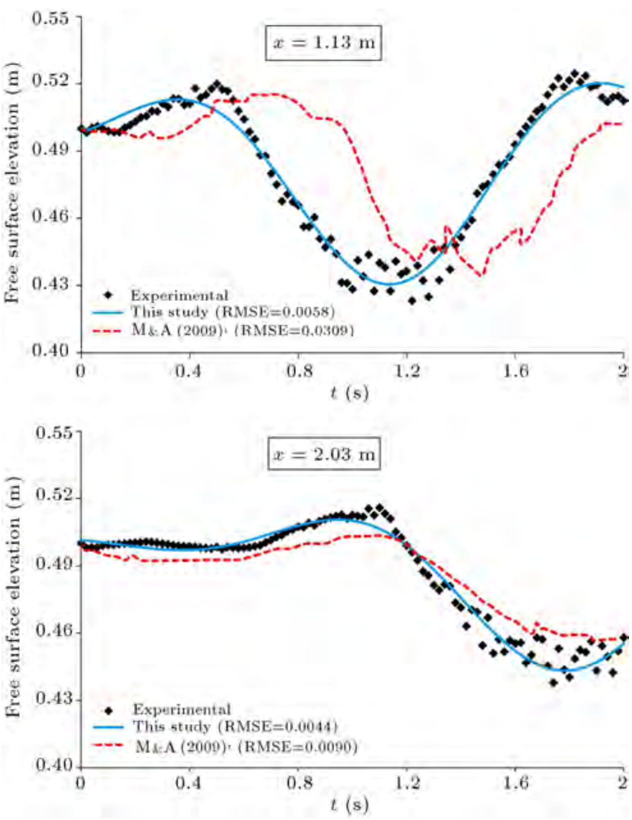

Figure 14. Experimental and computational time history of free surface elevation, case 4.

The predicted wave by LBM has slightly more speed, which may be due to existing friction between the block and surface of the beach. The amplitude of the first trailing is a little under-predicted, which is possibly caused by using a coarse resolution of lattices. The figure points out that the calculated wave by SPH has a considerable phase lag and smaller amplitudes, exhibiting a dissipative manner.

Velocity fields with vectors along the x-axis at different times are shown in Figure 15. While the block slides down, water overtops and pushes the block to the right side. Also a counterclockwise vortex is observed on top of the block, which moves upwards and dissipates during the course of sliding.

Figure 16 presents the velocity field and vectors over a plane cutting the y-axis at $y = 0.43$ m. Half the

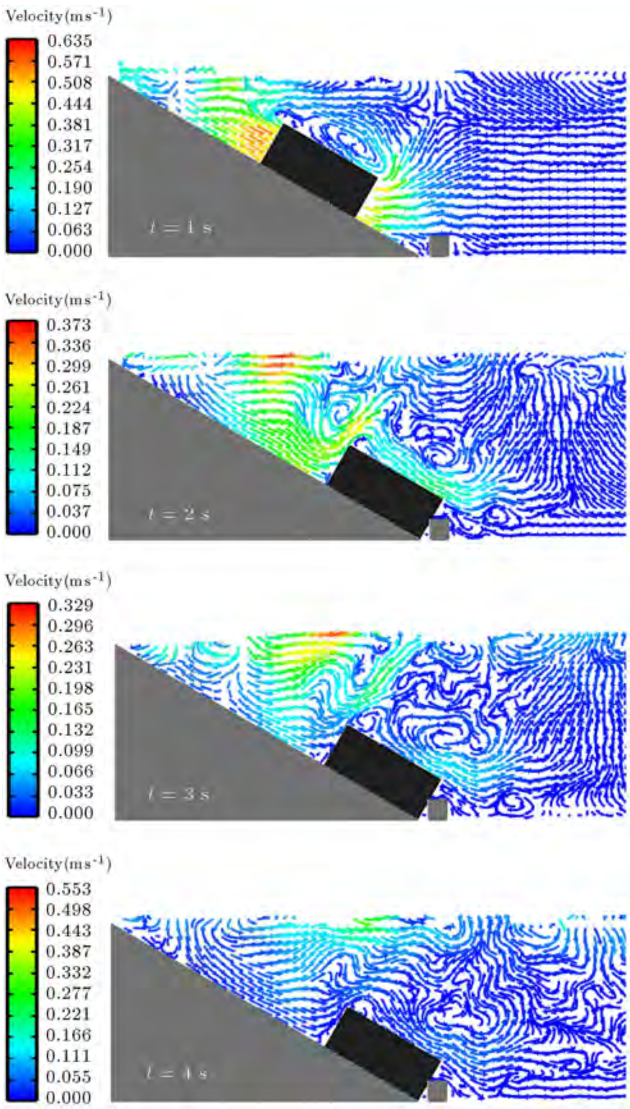

Figure 15. Velocity field with vectors along x-axis at different times, case 4.

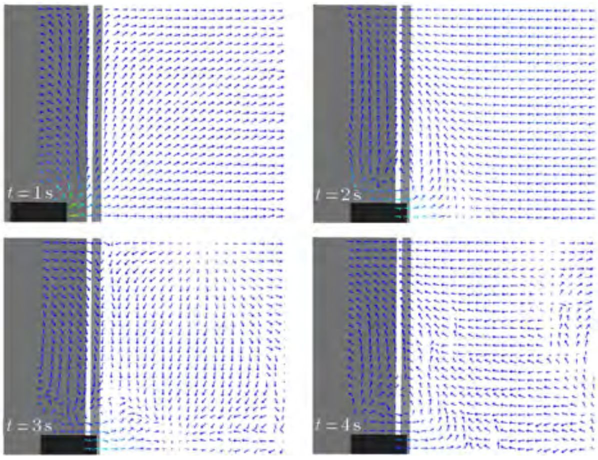

Figure 16. Velocity field with vectors at $y = 0.43$ m for different times, case 4.

domain is shown due to its symmetry. It is observed that a strong 3D wave generation and propagation pattern exists. By sliding the block, counterclockwise vortexes appear near the top side of the block, which are advected towards the flume walls. The figure exhibits a very complex flow field in the 3D case, which needs further investigations.

4. Conclusion

In this work, a novel approach, based on the Lattice Boltzmann Method (LBM), incorporated with the WALE turbulence model, was introduced to simulate impulsive waves generated by landslides, which is a complex problem regarding the free surface. The proposed LBM code takes the coupling between the motion of the landslide and variation of the flow field into account to predict the propagated impulsive waves. Validation of the LBM code was carried out by simulating a 2D submerged aerial, and a 3D submerged rigid landslide. The predicted results showed good agreement with recorded data. The LBM results were more accurate, in comparison with the Eulerian and SPH schemes, in predicting the amplitude and phase of the generated impulsive wave. The beneficial characteristics of LBM coding (simple formulation, easy coupling interaction, and stable and non-challenging numerical discretization) can overcome and eliminate Eulerian and SPH difficulties for accurate modeling of complex and non-linear interaction between the generated wave and the sliding obstacle. Extension of this work would be advantageous to wave-structure interaction problems in offshore and coastal frameworks which is currently in the authors' research program.

References

1. Heinrich, P. "Nonlinear water waves generated by submarine and aerial landslides", *Journal of Waterways, Ports, Coastal and Ocean Engineering*, **118**(3), pp. 249-266 (1992).
2. Walder, J.S., Watts, P., Sorensen, O.E. and Janssen, K. "Tsunami generated by subaerial mass flows", *Journal of Geophysical Research*, **28**, pp. 397-400 (2001).
3. Fritz, H.M., Hager, W.H. and Minor H.E. "Near field characteristics of landslide generated impulse waves", *Journal of Waterways, Ports, Coastal and Ocean Engineering*, **130**(6), pp. 287-302 (2004).
4. Grilli, S.T. and Watts, P. "Tsunami generation by submarine mass failure; Part I: Modeling, experimental validation and sensitivity analysis", *Journal of Waterways, Ports, Coastal and Ocean Engineering*, **131**(6), pp. 283-297 (2005).
5. Panizzo, A., Girolamo, P.D., Di Risio, M., Maistria, A. and Petaccia, A. "Great landslide events in Italian artificial reservoirs", *Journal of Natural Hazards and Earth System Sciences*, **5**, pp. 733-740 (2005).
6. Ataie, B. and Najafi, A. "Laboratory investigations on impulsive waves caused by underwater landslide", *Coastal Engineering*, **55**, pp. 989-1004 (2008).
7. Rzadkiewicz, S., Mariotti, C. and Heinrich, P. "Numerical simulation of submarine landslides and their hydraulic effects", *Journal of Waterways, Ports, Coastal and Ocean Engineering*, **123**(4), pp. 149-157 (1997).
8. Titov, V.V. "Numerical modeling of long wave runup", Ph.D. Thesis, University of Southern California, (1997).
9. Imran, J., Parker, G., Lacat, J. and Lee, H. "1D numerical model of muddy sub-aqueous and subaerial debris flows", *Journal of Hydraulic Engineering*, pp. 959-968 (2001).
10. Pak, A. and Sarfaraz, M. "Numerical study of the characteristics of surface waves generated by submarine landslides", *9th International Congress on Civil Engineering*, Isfahan, Iran (2012).
11. Janssen, C. and Krafczyk, M. "A Lattice Boltzmann approach for free-surface-flow simulations on non-uniform block-structured grids", *Journal of Computers and Mathematics with Applications*, **59**, pp. 2215-2235 (2010).
12. Sarfaraz, M. "Numerical analysis of concrete armor layers' stability in rubble-mound breakwaters", M.Sc. thesis, Sharif University of Technology, Tehran, Iran (2012).
13. Jie, T. and Xubo, Y. "Physically-based fluid animation: a survey", *Journal of Science in China Series F: Information Sciences*, **52**(1), pp. 1-17 (2009).
14. Monaghan, J.J. and Kos, A. "Scott Russell's wave generator", *Journal of Physics of Fluids*, **12**(3), pp. 622-630 (2000).
15. Gotoh, H., Sakai, T. and Hayashi, M. "Lagrangian two-phase flow model for the wave generation process due to large-scale landslides", *Asian and Pacific Coastal Engineering*, pp. 176-185 (2001).

16. Lo, E.Y.M. and Shao, S. "Simulation of near-shore solitary wave mechanics by an incompressible SPH method", *Journal of Applied Ocean Research*, **24**, pp. 275-286 (2002).

17. Shao, S.D. and Lo, E.Y.M. "Incompressible SPH method for simulating Newtonian and non-Newtonian flows with a free surface", *Journal of Advances in Water Resources*, **26**(7), pp. 787-800 (2003).

18. Shao, S.D. and Gotho, H. "Turbulence particle models for tracking free surfaces", *Journal of Hydraulic Research*, **43**(3), pp. 276-289 (2005).

19. Ataie, B. and Shobeyri, G. "Numerical simulation of landslide impulsive waves by incompressible smoothed particle hydrodynamics", *International Journal of Numerical Methods in Fluids*, **56**, pp. 209-232 (2008).

20. Mansour-Rezaei, S. and Ataie, B. "Compressible smoothed particle hydrodynamics for numerical simulation of impulsive waves", (in Farsi), *Iranian Journal of Hydraulics*, **4**(1), pp. 63-73 (2009).

21. Müller, M., Charypar, D. and Gross, M. "Particle-based fluid simulation for interactive applications", *Proceeding of the ACM SIGGRAPH/Eurographics Symposium on Computer Animation*, Switzerland, pp. 154-159 (2003).

22. Crespo, A.J.C. "Application of the smoothed particle hydrodynamics model SPHysics to free-surface hydrodynamics", Ph.D. Thesis, University of De Vigo, Italy (2008).

23. Yim., S.C., Yuk, D., Panizzo, A., Di Risio, M. and Liu, P.L.F. "Numerical simulation of wave generation by a vertical plunger using RANS and SPH models", *Journal of Waterways, Ports, Coastal, and Ocean Engineering*, **134**(3), pp. 1-17 (2008).

24. Ghassemi, A. and Pak, A. "Numerical study of factors influencing relative permeabilities of two immiscible fluids flowing through porous media using lattice Boltzmann method", *Journal of Petroleum Science and Engineering*, **72**, pp. 135-145 (2013).

25. Chen, C. and Doolen, G.D. "Lattice Boltzmann method for fluid flows", *Journal of Annual Review of Fluid Mechanics*, **30**, pp. 329-364 (1998).

26. Strumolo, G. and Viswanathan, B. "New directions in computational aerodynamics", *Journal of Physics and World*, **10**, pp. 45-49 (1997).

27. Liao, Q. and Jen, T.C. "Application of lattice Boltzmann method in fluid flow and heat transfer", *Computational Fluid Dynamics Technologies and Applications*, Edited by Minin, I.V. and Minin, O.V., Published by Intech, pp. 29-68 (2011).

28. Succi, S., *The lattice Boltzmann Equation for Fluid Dynamics and Beyond*, Clarendon Press, Oxford (2001).

29. Dazhi, Y., Mei, R., Luo, L.S. and Shyy, W. "Viscous flow computations with the method of lattice Boltzmann equation", *Journal of Progress in Aerospace Sciences*, **39**, pp. 329-367 (2003).

30. Lou, L.S. "Theory of the lattice Boltzmann method: Lattice Boltzmann models for non-ideal gases", *Journal of Physical Review*, **E62**, pp. 4982-4996 (2000).

31. Garnier, E., Adams, N. and Sagaut, P., *Large Eddy Simulation for Compressible Flows*, Springer (2009).

32. Weickert, M., Teike, G., Schmidt, O. and Sommerfeld, M. "Investigation of the LES WALE turbulence model within the lattice Boltzmann framework", *Journal of Computes and Mathematics with Applications*, **59**, pp. 2200-2214 (2010).

33. Hou, S., Sterling, J., Chen, S. and Doolen, G.D. "A lattice Boltzmann subgrid model for high Reynolds number flows", *Fields Institute Communications*, **6**, pp. 151-165 (1996).

34. Gunstensen, A.K., Rothman, D.H., Zaleski, S. and Zanetti, G. "Lattice Boltzmann model of immiscible fluids", *Journal of Physical Review*, **43**(8), pp. 4320-4327 (1991).

35. Ginzburg, I. and Steiner, K. "A free-surface lattice Boltzmann method for modelling the filling of expanding cavities by Bingham fluids", *Journal of Philosophical Transactions: Mathematical, Physical and Engineering Sciences*, **360**, pp. 453-466 (2002).

36. Körner, C., Thies, M., Hofmann, T., Thürey, N. and Rüde, U. "Lattice Boltzmann model for free surface flow for modeling foaming", *Journal of Statistical Physics*, **121**, pp. 179-196 (2005).

37. Thürey, N. "Physically based animation of free surface flows with the lattice Boltzmann method", Ph.D. Thesis, University of Erlangen-Nürnberg, Bavaira, Germany (2007).

38. Ziegler, D.P. "Boundary conditions for lattice Boltzmann simulations", *Journal of Statistical Physics*, **71**, pp. 1171-1177 (1993).

39. Next Limit Inc. "XFlow user's manual", Madrid, Spain (2012).

Biographies

Ali Pak is Professor of Civil Engineering at Sharif University of Technology, Tehran, Iran. He has extensive publications in various fields of engineering, such as numerical modeling of soil structures, petroleum geomechanics, environmental geotechnics, liquefaction modeling, and hydraulic fracturing.

Mohammad Sarfaraz obtained a BS degree in Civil Engineering from the Power and Water University of Technology, Iran, in 2010, and an MS degree in Geotechnical Engineering from Sharif University of Technology, Tehran, Iran, in 2012. He ranked first among all students both in BS and MS programs. His main research interests include: wave-structure interaction, coastal and offshore structures, geotechnical earthquake engineering, lattice Boltzmann Method, and impulsive water waves generated by landslides.